A Model for Diffusive Transport through a Spherical Interface Probed by Pulsed-Field Gradient NMR

William S. Price,* Alexander V. Barzykin,# Kikuko Hayamizu,# and M. Tachiya#
*Water Research Institute, and #National Institute of Materials and Chemical Research, Tsukuba, Ibaraki 305, Japan

ABSTRACT In biological systems, because of higher intracellular viscosity and/or the restriction of the diffusion space inside cells, the (apparent) diffusion coefficient of an intracellular species (e.g., water) is generally smaller than when it is in the extracellular medium. This difference affects the spin-echo signal attenuation in the pulsed field gradient NMR experiment and thus affords a means of separating the intracellular from the extracellular species, thereby providing a basis for studying transmembrane transport. Such experiments have commonly been analyzed using the macroscopic model of Kärger (see *Adv. Magn. Reson.* 21:1–89 (1988)). In our previous study, we considered a microscopic model of diffusive transport through a spherical interface using the short gradient pulse approximation (*J. Magn. Reson.* A114:39–46 (1995)). The spins in the external medium were modeled with the "partially absorbing wall" condition or as having a small but finite lifetime. In the present paper, we extend our treatment to the case in which there is no limitation upon the lifetime in either medium. We also consider a simple modification of Kärger's model that more properly accounts for the restricted intracellular diffusion. Importantly, it was found that the exact solution within the short gradient pulse approximation developed here and the modified Kärger model are in close agreement in the (experimentally relevant) long-time limit. The results of this study show that when there is no limitation upon the lifetime of the transported species in either phase, the spin-echo attenuation curve is very sensitive to transport.

INTRODUCTION

Transport and interdomain exchange are extremely important in micellar and vesicular catalysis and for all biological systems (Zwanzig and Szabo, 1991; Barzykin and Tachiya, 1996). Because of its noninvasive nature, NMR spectroscopy is one of the most powerful techniques of studying transport in biological systems. Traditional NMR methods, such as inversion transfer and saturation transfer (Price and Kuchel, 1990b; Kuchel, 1990), rely upon a difference in the chemical shift or the relaxation rate to distinguish between the exchanging sites. In many cases, such differences do not exist or they are very small (e.g., water). However, there are generally differences in the diffusion coefficient and in the available diffusion space for the probe molecule between the intra- and extracellular compartments (e.g., Price et al., 1989a,b; Price and Kuchel, 1990b; Price et al., 1992). Such differences may be exploited with pulsed field gradient nuclear magnetic resonance (PFG NMR, also referred to as pulsed gradient spin-echo or PGSE NMR; Kärger et al., 1988; Stilbs, 1987; Callaghan, 1991; Price, 1996, 1997) to separate the domains (Andrasko, 1976; Price and Kuchel, 1990b; Van Zijl et al., 1991; Potter et al., 1996), even in the absence of chemical shift and/or relaxation rate differences. The exchange modulates the diffusion in both domains and thus, ultimately, the attenuation of the spin-echo signal. Generally the permeability coefficients are very small. For example, the "effective" values reported in the literature for bicarbonate permeability across the red blood cell membrane range from 4×10^{-7} to 3×10^{-6} m s^{-1} (Kuchel et al., 1987; Chapman et al., 1986). Yet bicarbonate is one of the fastest transporting species known for the red blood cell.

PFG NMR, with a displacement sensitivity of ~100 nm and a lower limit for measuring diffusion coefficients of $\sim 10^{-14}$ m^2 s^{-1} (Callaghan, 1984), provides an excellent tool for probing molecular diffusion and structure in biological systems, and is especially convenient because it does not require labeled probe molecules; they are either used "as is" or after isotopic enrichment (e.g., ^{13}C). Consequently, no thermodynamic gradients are introduced. PFG has also been used in biological systems to study binding and molecular association (e.g., Lennon et al., 1994; Andreasson et al., 1996; Wassall, 1996; Krishnan, 1997; Price et al., 1997b; Price, 1998a). PFG has numerous other NMR applications, including solvent suppression, phase cycling, and imaging (e.g., Price, 1996, 1998b; Price and Arata, 1996; Price et al., 1997a).

The aim of the present paper is to develop more cogent models for analyzing PFG NMR data to extract information on diffusion and, particularly, exchange through spherical interfaces. In the following section, the basis of PFG NMR diffusion measurements in free solution and in the case in which the diffusion is restricted by a spherical interface is briefly explained. Next, the commonly used simple two-site macroscopic model of Kärger (Kärger et al., 1988) is reviewed, and a modification more in keeping with the problem at hand is presented. As will be elucidated below, the starting premise of the two-site Kärger model does not consider the effects of restricted diffusion (i.e., it is assumed that there is free diffusion in both domains). Consequently,

Received for publication 27 October 1997 and in final form 20 January 1998.

Address reprint requests to Dr. William S. Price, Water Research Institute, Sengen 2-1-6, Tsukuba, Ibaraki 305-0047, Japan. Tel.: 81-298-58-6186; Fax: 81-298-58-6144; E-mail: wprice@wri.co.jp.

0006-3495/98/05/2259/13 $2.00

we attempt to develop a model that is more consistent with the microscopic reality of the two-site exchange problem. The full solution for the "microscopic" approach is mathematically complex, and we develop our solution after first considering the related but mathematically simpler problem of the pseudo-one-site "partially absorbing wall" model and our recently derived extension to this model, which accounted for a small but finite lifetime in the extracellular phase (Barzykin et al., 1995). The model that we ultimately develop in the present paper contains no limitation on the relative lifetimes in either domain. The "microscopic" approach and the modified Kärger models that are developed in this paper are compared.

THEORY

PFG NMR diffusion measurements

The theory behind the PFG method has recently been presented in detail (Price, 1997). Briefly, the PFG spin-echo pulse sequence is a modification of the Hahn spin-echo pulse sequence, in which typically a "rectangular" magnetic field gradient pulse of duration δ and magnitude g is inserted into each τ period (see Fig. 1). The separation between the leading edges of the gradient pulses is denoted by Δ and constitutes the time over which diffusion is measured. If a spin moves along the direction of the field gradient during Δ, the phase change exerted by the first gradient pulse is not cancelled by the phase change exerted by the second (NB identical) gradient pulse. This phase shifting effect, when averaged over an ensemble of spins, leads to a diminution of the signal, which is proportional to the net displacement of the spin along the direction of the gradient during Δ and the magnitude of the gradient. In a solution state PFG NMR experiment, typical gradient magnitudes range from ~0.10 to 20 Tm^{-1}. Generally Δ is kept constant, with its minimum value being limited by the effects of gradient pulse induced eddy currents, and the upper limit being set by the transverse relaxation times (i.e., the PFG sequence is based on a Hahn spin echo) of the observed species. Operationally this corresponds to values in the range of ~5–200 ms. δ is typically varied from 0 to 20 ms.

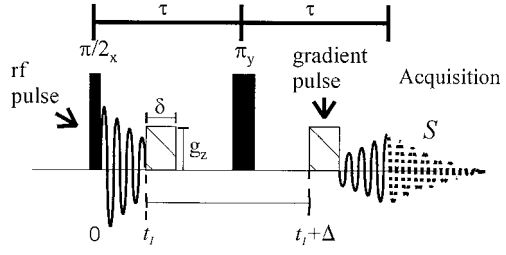

FIGURE 1 The pulsed field gradient NMR sequence. The sequence is a Hahn spin-echo pulse sequence with the addition of two identical gradient pulses of duration, δ, and magnitude, g, with one gradient pulse being inserted in each τ period. The time over which diffusion is measured is denoted by Δ and corresponds to the time between the leading edges of the gradient pulses. The second half of the echo is digitized and used as the FID (i.e., the signal, S). The attenuation, E, of the spin-echo signal is obtained by normalizing the amplitude of the spin-echo signal by the amplitude of the spin-echo signal under zero gradient conditions. The normalization removes the relaxation dependence on the transverse relaxation that occurs during the pulse sequence. Diffusion is measured along the direction of the gradient pulses.

Ideally, an analytical solution relating the echo attenuation (E) to the experimental variables would be derived from the Bloch equations modified to include the effects of diffusion (Torrey, 1956; Stejskal and Tanner, 1965; Caprihan et al., 1996; Price, 1997); however, in practice this approach is mathematically intractable, and various approximations (Caprihan et al., 1996; Price, 1997) or even numerical methods must be resorted to. In the present work we consider the commonly used short gradient pulse (SGP) approximation, where motion during the gradient pulse is ignored (rigorously, one assumes that $\delta \rightarrow 0$ and $|\mathbf{g}| \rightarrow \infty$ while their product remains finite), although, as can be seen from above, the experimental conditions often violate this condition. In the SGP approximation the PFG spin-echo attenuation is given by (Stejskal, 1965)

$$E(\mathbf{q}, \Delta) = \int\int d\mathbf{r}_0\, d\mathbf{r}\, \rho(\mathbf{r}_0) G(\mathbf{r}_0|\mathbf{r}; \Delta) e^{i\mathbf{q}\cdot(\mathbf{r}-\mathbf{r}_0)}, \quad (1)$$

where $\mathbf{q} = \gamma\delta\mathbf{g}$, γ is the gyromagnetic ratio, and $\rho(\mathbf{r}_0)$ is the equilibrium spin density. Usually the spin-echo amplitude is normalized to the echo amplitude under zero gradient conditions. The normalization removes the dependence on the transverse relaxation that occurs during the Hahn spin-echo pulse sequence. This normalization assumes that all spins suffer the same degree of transverse relaxation in the course of the pulse sequence. The effects of any relaxation correlated with translational motion are ignored.

The Green's function (or diffusion propagator), $G(\mathbf{r}_0|\mathbf{r}; \Delta)$ (sometimes denoted by $P(\mathbf{r}_0|\mathbf{r}; \Delta)$, although not to be confused with the Legendre polynomial), is the conditional probability that a spin starting at position $\mathbf{r}_0$ will migrate to $\mathbf{r}$ in a time Δ. $G(\mathbf{r}_0|\mathbf{r}; \Delta)$ satisfies the diffusion equation

$$\frac{\partial G(\mathbf{r}_0|\mathbf{r}; t)}{\partial t} = D\nabla^2 G(\mathbf{r}_0|\mathbf{r}; t), \quad (2)$$

where ∇^2 denotes the Laplacian operator, subject to the initial condition

$$G(\mathbf{r}_0|\mathbf{r}; 0) = \delta(\mathbf{r} - \mathbf{r}_0), \quad (3)$$

where δ is the Dirac δ function (not to be confused with the time interval δ), and the appropriate boundary conditions. From Eq. 1 it can be realized that there is a Fourier relationship between $E(\mathbf{q}, \Delta)$ and the spectrum of the displacement of the spins (Kärger and Heink, 1983). Thus in the PFG NMR experiment, $\tilde{\mathbf{q}} = \mathbf{q}/2\pi$ is the equivalent of the wavevector used in x-ray diffraction (Cory and Garroway, 1990; Callaghan et al., 1991; Callaghan and Coy, 1992).

For the case of free diffusion the propagator is Gaussian:

$$G(\mathbf{r}_0|\mathbf{r}; t) = (4\pi D t)^{-3/2} e^{-[(\mathbf{r}-\mathbf{r}_0)^2]/4Dt}, \quad (4)$$

and the solution to Eq. 1 has a particularly simple form, given by

$$E(q, \Delta) = \exp(-q^2 D\Delta), \tag{5}$$

where $q = |\mathbf{q}|$. We remark that, because the solution given by Eq. 5 is for the SGP limit, the $-\delta/3$ correction term for Δ (Stejskal and Tanner, 1965; Price, 1997) is absent.

Restricted diffusion

Typical radii for biological "spherical" interfaces range from ~12 nm for small unilamellar vesicles (New, 1990) to ~3 μm (the "effective" radii of a human red blood cell), and the diffusion coefficients of small rapidly transported species are in the range of 10^{-9} to 10^{-10} m^2 s^{-1}; such a system is schematically depicted in Fig. 2 *A*. In the case of free diffusion, the mean square displacement can be determined from Eq. 4 to be

$$\langle(\mathbf{r} - \mathbf{r}_0)^2\rangle = 6Dt. \tag{6}$$

Thus from Eq. 6 and considering the time-scale over which the PFG diffusion measurements are conducted (i.e., Δ = 10 ms to 1 s), it can be seen that the diffusion of small molecules inside biological interfaces is restricted.

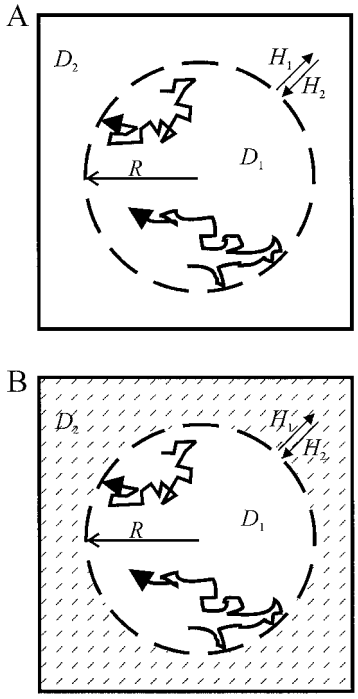

FIGURE 2 Schematic representation of a spherical biological interface in which a species in the external medium is modeled (*A*) as having infinitely fast relaxation (i.e., no external lifetime) and (*B*) finite lifetime. When spins in the external medium have infinitely short (NMR visible) lifetimes, the ratio of the internal to external concentrations can be neglected, and only the internal diffusion coefficient, D_1, and the permeability, H_1, are relevant. When the spins in the external medium have finite lifetime, the ratios of the internal to external concentration, diffusion coefficient, and permeabilities are needed to describe the system. It is convenient to define the reduced permeability coefficient, $h = HR/D$.

When the diffusion is restricted, the propagator is no longer Gaussian, the mean square displacement no longer scales linearly with time, and, consequently, a more complicated equation than Eq. 5 relates the echo attenuation to D and the experimental variables. Although this makes the analysis of data from the PFG experiment more cumbersome, the data now also contain structural information on the restricting interface (Price, 1997). In the ideal case, one experiment may be used to provide the diffusion coefficient and the exchange rate of the transporting species, together with the topology of the domains (e.g., cell and vesicle shape) between which they are transported. When diffusion is restricted to a sphere of radius R, the relationship between the experimental variables and the echo attenuation is given by (Balinov et al., 1993)

$$E(q, \Delta) = \left[\frac{3j_1(a)}{a}\right]^2 + 6a^2 \sum_{n=0}^{\infty} j_n'(a)^2 \sum_{m=0}^{\infty} \frac{(2n+1)\alpha_{nm}^2}{\alpha_{nm}^2 - n^2 - n} \exp(-\alpha_{nm}^2 \xi) \frac{1}{[\alpha_{nm}^2 - a^2]^2}, \tag{7}$$

where $\xi = D\Delta/R^2$, $a = qR$, α_{nm} is the mth nonzero root of the equation

$$j_n'(\alpha) = 0, \tag{8}$$

and $j_n(x)$ is the spherical Bessel function of the first kind (e.g., see Abramowitz and Stegun, 1970). From the above discussion it can be seen that in most experimental circumstances we are in the "long time limit," such that the condition $\xi > 1$ holds. When $\xi \gg 1$, Eq. 7 reduces to

$$E(q, \Delta) = \left[\frac{3j_1(a)}{a}\right]^2. \tag{9}$$

This has the physical interpretation that during the experiment (i.e., Δ), all of the spins feel the effects of the restricting boundary equally, and the echo signal attenuation loses its diffusional dependence and becomes a function of $a = qR$ only (i.e., Eq. 9).

In analyzing the PFG dependencies for restricted geometries, one often implies an analogy to the free diffusion case and defines an apparent diffusion coefficient by

$$D_{app}(\Delta) = -\frac{1}{\Delta} \lim_{q \to 0} \frac{\partial \ln[E(q, \Delta)]}{\partial[q^2]}. \tag{10}$$

Consequently, the presence of restricted diffusion is often noted by a lower (apparent) diffusion coefficient.

Two-site Kärger model

By noting the apparent lowering of the diffusion coefficient in a restricted system when the data are analyzed with the

free diffusion model (i.e., Eqs. 5 and 10), it can be conjectured that exchange through a spherical interface can be determined by using the difference between the real and apparent diffusion coefficients in the external and internal domains. The theory for molecular transport and exchange in composed systems has been presented by Kärger and co-workers (e.g., see Kärger et al., 1988). In the Kärger model, it is assumed that the exchanging species undergoes free diffusion in each of the two equivalent domains. In analyzing the case of exchange through a spherical interface, one domain is normally referred to as the internal phase and the other as the external phase.

The two-site Kärger model is derived starting from the coupled differential equations describing the echo signal intensities for the internal phase (denoted by the subscript 1),

$$\frac{dE_1}{dt} = -q^2 D_1 E_1 - \frac{E_1}{\tau_1} + \frac{E_2}{\tau_2}, \tag{11}$$

and the external phase (denoted by the subscript 2),

$$\frac{dE_2}{dt} = -q^2 D_2 E_2 - \frac{E_2}{\tau_2} + \frac{E_1}{\tau_1}, \tag{12}$$

with the initial conditions

$$E_1(q, 0) = P_1, E_2(q, 0) = P_2 \tag{13}$$

and

$$\left.\frac{dE_2(q, t)}{dt}\right|_{t=0} = -q^2 D_2 P_2, \left.\frac{dE_1(q, t)}{dt}\right|_{t=0} = -q^2 D_1 P_1. \tag{14}$$

The solution to these equations is given by

$$E(q, \Delta) = C_A e^{-q^2 D_A \Delta} + C_B e^{-q^2 D_B \Delta}, \tag{15}$$

where D_A and D_B are the apparent self-diffusion coefficients defined below, and C_A and C_B are the population fractions (relative signal intensities):

$$D_{A,B} = \frac{1}{2}\left\{D_1 + D_2 + \frac{1}{q^2}\left(\frac{1}{\tau_1} + \frac{1}{\tau_2}\right) \mp \sqrt{\left[D_1 - D_2 + \frac{1}{q^2}\left(\frac{1}{\tau_1} - \frac{1}{\tau_2}\right)\right]^2 + \frac{4}{q^4 \tau_1 \tau_2}}\right\}, \tag{16}$$

$$C_A = 1 - C_B, \tag{17}$$

and

$$C_B = \frac{P_1 D_1 + P_2 D_2 - D_A}{D_B - D_A}, \tag{18}$$

and D_1 and D_2 are the diffusion coefficients in the two domains. Similarly, P_1 and P_2 are the relative populations and τ_1 and τ_2 (not to be confused with the τ delay in the PFG pulse sequence; see Fig. 1) are the mean residence lifetimes in each compartment. Thus the effect of diffusion on the signal intensity when transport occurs between two freely diffusing regions (ignoring relaxation time differences between the two compartments) is given by a superposition of exponentials (Kärger et al., 1988). A number of simplifications are available (Kärger et al., 1988; Waldeck et al., 1997). Some applications of this model to experimental systems have recently been reviewed (Waldeck et al., 1997).

Modified two-site Kärger model

As noted above, the internal site is in reality restricted (see Fig. 2 *A*), and the condition $\xi > 1$ generally holds. Consequently, the signal intensity of the internal component does not depend on the diffusion coefficient of the internal species and is, instead, only a function of qR (i.e., Eq. 9). In our modification to the Kärger model the effects of restriction in the internal domain are approximately accounted for. Thus, more realistically, Eq. 11 should be replaced by

$$\frac{dE_1}{dt} = -\frac{E_1}{\tau_1} + \frac{E_2}{\tau_2}, \tag{19}$$

and, noting from above the long time limit formula for attenuation within a sphere (i.e., Eq. 9), the initial conditions for $E_1(t)$ now become

$$E_1(q, 0) = P_1\left[\frac{3j_1(a)}{a}\right]^2 = \widehat{P}_1 \quad \text{and} \quad \left.\frac{dE_1(q, t)}{dt}\right|_{t=0} = 0 \tag{20}$$

Thus the attenuation at time $t = \Delta$ takes the same form as Eq. 15, but with

$$C_A = P_2 + \widehat{P}_1 - \frac{D_2 P_2 - D_1 P_2 - D_A \widehat{P}_1}{(D_B - D_A)}, \tag{21}$$

$$C_B = \frac{D_2 P_2 - D_A P_2 - D_A \widehat{P}_1}{(D_B - D_A)} \tag{22}$$

and

$$D_A, D_B = \frac{1}{2}\left\{D_2 + \frac{1}{q^2}\left(\frac{1}{\tau_1} + \frac{1}{\tau_2}\right) \mp \sqrt{\left[D_2 - \frac{1}{q^2}\left(\frac{1}{\tau_1} - \frac{1}{\tau_2}\right)\right]^2 + \frac{4}{q^4 \tau_1 \tau_2}}\right\}. \tag{23}$$

The modified Kärger model is very similar to the original Kärger model presented in the previous section, and the exponential term in the Kärger model reduces to that of the modified model if the diffusion coefficient in the restricted medium is set to 0 (i.e., $D_1 = 0$). The preexponential factors (i.e., Eqs. 21 and 22) are, however, quite different.

Equation 23 can be further simplified. In the slow exchange limit (i.e., $\tau_1, \tau_2 \to \infty$) we have

$$D_A \approx \frac{1}{q^2 \tau_1} \tag{24}$$

and

$$D_B \approx D_2 + \frac{1}{q^2\tau_2}. \quad (25)$$

In the fast exchange limit (i.e., $\tau_1, \tau_2 \to 0$) we only need to consider D_A (because $D_B \to \infty$, and thus the second term in Eq. 15 $\to 0$), and we obtain

$$D_A \approx \frac{\tau_1}{\tau_1 + \tau_2}. \quad (26)$$

Even allowing for this modification to better account for the reality of diffusion in one domain being subject to restricted diffusion, the Kärger approach still involves a serious approximation. In particular, there is no consideration of the starting point inside the sphere; thus there is the implicit assumption that exchanging spins sample all points of the sphere before being transported. Hence this approach is strictly only applicable to the case of very slow exchange. However, this approximation considerably simplifies the solution of the underlying diffusion problem, which is otherwise extremely complicated, even for a two-site system. The limitations of the macroscopic approach will be more fully discussed below.

One-site SGP model

Assuming that it is possible to obey the requirements for the SGP approximation, a more rigorously correct relationship between the transport and the experimental variables can be derived from Eqs. 1–3 by using the proper boundary conditions at the interface. Even when the SGP approximation is used, such a derivation is nontrivial, and a means of making the system more mathematically tractable is to manipulate the relaxation properties of the system to achieve the "partially absorbing wall" condition. In this case a two-site (i.e., domain) system is modeled by a one-site system implying infinitely fast relaxation in the outer domain (see Fig. 2 *B*).

Previous PFG NMR studies using the partially absorbing boundary condition have considered the case of diffusion in regions confined by planes and in porous media of different geometries (Frey et al., 1988; Mitra and Sen, 1992; Snaar and Van As, 1993; Sen et al., 1994; Coy and Callaghan, 1994; Callaghan, 1995). This situation is straightforwardly realized if the interface is covered by a layer of active relaxation centers or if relaxation agents are added to the exterior medium. The nuclear magnetization is then immediately annihilated upon transport to the exterior. This condition can also be met in the PFG experiment when the external spin diffusivity significantly exceeds the internal spin diffusivity. When the partially absorbing wall condition is met, we may confine our consideration to the molecules that do not leave the sphere. Once they have left, the spins will cover such large distances in the external medium that their contribution to the echo signal with increasing field gradient intensities rapidly drops to zero as a function of q. The corresponding partially absorbing boundary condition reads

$$D\frac{\partial G(\mathbf{r}_0|\mathbf{r}; t)}{\partial r} + HG(\mathbf{r}_0|\mathbf{r}; t)|_{r=R} = 0, \quad (27)$$

where $r = |\mathbf{r}|$ and H (ms^{-1}) is the permeability coefficient (or the density of the surface relaxation centers). It should be noted that the microscopic first-order rate constant for transport through a spherical interface can be related to the permeability as follows: $k_{tr} = 3H/R$ (Barzykin et al., 1995). Below we shall see that it is convenient to define the reduced permeability by $h = HR/D$. The use of the partially absorbing boundary condition turns a two-site problem into a pseudo-one-site problem.

The solution to the diffusion problem posed in Eqs. 2, 3, and 27, given rotational symmetry about the direction of the field gradient, is well known and is most conveniently written in terms of the corresponding eigenfunctions (Carslaw and Jaeger, 1959; Mitra and Sen, 1992),

$$G(r_0, \mu_0|r, \mu; t) = \frac{1}{2\pi R^3}\sum_{n,m=0}^{\infty}(2n+1)P_n(\mu_0)P_n(\mu) \times \exp\left(-\frac{Dt}{R^2}\alpha_{nm}^2\right)\frac{\alpha_{nm}^2 j_n(\alpha_{nm}r_0/R)j_n(\alpha_{nm}r/R)}{[h(h-1)+\alpha_{nm}^2 - n(n+1)]j_n^2(\alpha_{nm})}, \quad (28)$$

where $\mu_0 = \cos\theta_0$, $\mu = \cos\theta$ (the polar angles with respect to $\mathbf{g}$), and $P_n(\mu)$ are the Legendre polynomials, and α_{nm} are the positive roots of the equation

$$(n+h)j_n(\alpha_{nm}) = \alpha_{nm}j_{n+1}(\alpha_{nm}), \quad (29)$$

numbered by $m = 0, 1, \ldots$ in increasing order. The Fourier transform in Eq. 1 is readily carried out by using the addition theorem (Abramowitz and Stegun, 1970) to expand the complex exponential and noting that $\rho(\mathbf{r}_0) = 3/(4\pi R^3)$. The result is (Mitra and Sen, 1992)

$$E(q,\Delta) = 6\sum_{n,m=0}^{\infty}(2n+1)\frac{\exp(-\xi\alpha_{nm}^2)}{h(h-1)+\alpha_{nm}^2 - n(n+1)} \times \left\{\frac{\alpha_{nm}}{\alpha_{nm}^2 - a^2}[(n+h)j_n(a) - aj_{n+1}(a)]\right\}^2. \quad (30)$$

In a typical experiment (vide supra) the condition $\xi > 1$ holds, and only the lowest eigenvalue $\alpha = \alpha_{00}$ is important. It satisfies the following equation:

$$1 - h = \alpha\cot\alpha. \quad (31)$$

In this long-time limit the normalized echo amplitude is

independent of ξ and is given by

$$E(q, \Delta) = \left\{\frac{1}{h}\frac{\alpha^2}{\alpha^2 - a^2}\left[(h-1)\frac{\sin a}{a} + \cos a\right]\right\}^2. \quad (32)$$

In the limit of weak permeability (i.e., $h \to 0$, reflecting boundary), the lowest positive solution of Eq. 31 is $\alpha^2 = 3h$, and Eq. 32 transforms into (i.e., Eq. 9)

$$E(q, \Delta) = \left[\frac{3j_1(a)}{a}\right]^2 \quad \text{for } h \to 0, \quad (33)$$

whereas in the limit of infinite permeability (i.e., $h \to \infty$, perfectly absorbing boundary) we have

$$E(q, \Delta) = \left[\frac{\pi^2}{\pi^2 - a^2}\frac{\sin a}{a}\right]^2 \quad \text{for } h \to \infty. \quad (34)$$

In cell or vesicle systems, the partially absorbing wall experiment is practicable, at least in principle, as the relaxation properties of the exterior medium can easily be manipulated through the addition of relaxation agents such as Mn^{2+} ions. However, we have previously shown that it is experimentally difficult to attain the instant quenching condition (Price and Kuchel, 1990b; Barzykin et al., 1995). Moreover, it is generally undesirable to add foreign species, because they may affect and perhaps irreversibly change the system being studied. This is a high price to pay for mathematical simplicity, especially when the model is only weakly sensitive to transport (Mitra and Sen, 1992; Barzykin et al., 1995). Importantly, if the quenching condition is not completely met, the short-lived spins in the exterior medium, although possessing a higher mobility, still contribute considerably to the echo signal. This is particularly true when the motion of the spins in the extracellular medium are subject to obstruction, as would be expected in, for example, a high hematocrit suspension of red blood cells (i.e., the restricting geometries have a high volume fraction). We have further developed a two-site model for the more experimentally relevant case in which the spins have a short but finite lifetime upon transporting through the spherical interface (Barzykin et al., 1995). The theory is based on solving the diffusion equations for two domains coupled by appropriate boundary conditions.

Two-site SGP model

To take advantage of the one-site model for describing the interphase exchange, in the absence of relaxation agents, either the molecular mobility or the relaxation rate in one phase (i.e., the exterior) must significantly exceed those in the other phase (i.e., the interior). Normally the difference in diffusivity between the domains in a biological system is small. For example, the diffusion coefficient of the bicarbonate analog, hypophosphite, in water solution at 310 K has been found to be $\sim 1.6 \times 10^{-9}$ m^2 s^{-1} (Price and Kuchel, 1990b), whereas the diffusion coefficient in intact human red blood cells has been estimated to be about 6×10^{-10} m^2 s^{-1} from NMR relaxation measurements (Price et al., 1989b) and $\sim 1.5 \times 10^{-10}$ m^2 s^{-1} from PFG measurements (Price and Kuchel, 1990b). The true diffusion coefficient in the unconfined media may even be underestimated by the PFG measurement because of the effects of obstruction (Jönsson et al., 1986; Blees and Leyte, 1994). Hypophosphite is a particularly useful probe molecule for the present study, because in a red cell suspension there are separate peaks in the ^{31}P NMR spectrum for the internal and external species. Furthermore, the transport may be inhibited by the addition of dinitrostilbene (Price and Kuchel, 1990a).

In this section we present a more general formulation, explicitly including restricted diffusion of the particles in both domains, between which the transport is occurring. The main results are given below, and a detailed derivation is presented in the Appendix. In this model, as depicted schematically in Fig. 2 *A*, the two domains are characterized by different diffusion coefficients. The transverse relaxation time is assumed to be constant and thus is factored out for simplicity. We also neglect "many-body" effects that have been observed in PFG of emulsions (e.g., Van Den Enden et al., 1990; Fourel et al., 1994) and assume that any spin is involved with only one spherical compartment in the course of the experiment.

The Green's function satisfies the diffusion equation in each domain:

$$\frac{\partial G_{ij}(\mathbf{r}_0|\mathbf{r}; t)}{\partial t} = D_j \nabla^2 G_{ij}(\mathbf{r}_0|\mathbf{r}; t) \quad \text{for } i, j = 1, 2, \quad (35)$$

where the first subscript of G_{ij} indicates whether the initial position of the particle is inside ($i = 1$, $r_0 \le R$) or outside ($i = 2$, $r_0 \ge R$) the sphere, and the second subscript bears information on the current spatial coordinate r. The boundary conditions are given by

$$D_1 \left.\frac{\partial G_{i1}}{\partial r}\right|_{r=R} = D_2 \left.\frac{\partial G_{i2}}{\partial r}\right|_{r=R} \quad (36)$$

and

$$D_1 \frac{\partial G_{i1}}{\partial r} + H_1 G_{i1} - H_2 G_{i2}|_{r=R} = 0 \quad \text{for } i = 1, 2. \quad (37)$$

Equation 36 describes the flux continuity over the interface, and Eq. 37 states that the flux is proportional to the difference in spin concentration between the domains weighted with the appropriate permeability coefficients. At equilibrium, there is no net flux across the interface, and

$$[G_{i1}/G_{i2}]_{eq} = C_1/C_2 = H_2/H_1 = K, \quad (38)$$

where C_1 and C_2 are the concentrations of the particles in domains 1 and 2, respectively.

We follow the standard procedure (Carslaw and Jaeger, 1959) in deriving the Green's function for the posed diffusion problem. We obtain for the Laplace transform of the

relevant Green's function for spins starting from inside the sphere (A. V. Barzykin and M. Tachiya, 1998)

$$\hat{G}_{11}(r_0, \mu_0|r, \mu; \epsilon) = \frac{s_1}{2\pi^2 D_1} \sum_{n=0}^{\infty}(2n+1)P_n(\mu_0)P_n(\mu)i_n(s_1 r_<) \times \left[k_n(s_1 r_>) + \frac{\Lambda_n^{kk}}{\Lambda_n^{ik}} i_n(s_2 r_>)\right], \quad (39)$$

$$\hat{G}_{12}(r_0, \mu_0|r, \mu; \epsilon) = \frac{h_1}{4\pi D_2 R} \sum_{n=0}^{\infty}(2n+1)P_n(\mu_0)P_n(\mu) \times \frac{i_n(s_1 r_0)k_n(s_2 r)}{\Lambda_n^{ik}}, \quad (40)$$

and for spins starting from outside the sphere:

$$\hat{G}_{22}(r_0, \mu_0|r, \mu; \epsilon) = \frac{s_2}{2\pi^2 D_2} \times \sum_{n=0}^{\infty}(2n+1)P_n(\mu_0)P_n(\mu)k_n(s_2 r_>) \times \left[i_n(s_2 r_<) + \frac{\Lambda_n^{ii}}{\Lambda_n^{ik}} k_n(s_2 r_<)\right], \quad (41)$$

whereas from detailed balance,

$$G_{21} = KG_{12}, \quad (42)$$

where $i_n(x)$ and $k_n(x)$ are the modified spherical Bessel functions (Abramowitz and Stegun, 1970), $s_1 = \sqrt{\epsilon/D_1}$, $s_2 = \sqrt{\epsilon/D_2}$, and $r_< = \min(r, r_0)$, $r_> = \max(r, r_0)$. The Laplace transform is defined by

$$\hat{G}(\epsilon) = \int_0^{\infty} e^{-\epsilon t} G(t) \mathrm{d}t. \quad (43)$$

The coefficients $\Lambda_n^{\sigma\upsilon}(\lambda)$ are determined from the boundary conditions to be

$$\Lambda_n^{\sigma\upsilon}(\lambda) = \phi_n^{\sigma}(\lambda)\phi_n^{\upsilon}(\eta\lambda) - (-1)^{\delta_{\sigma,i}} h_1 \sigma_n(\lambda)\phi_n^{\upsilon}(\eta\lambda) + (-1)^{\delta_{\upsilon,i}} h_2 \phi_n^{\sigma}(\lambda)\upsilon_n(\eta\lambda), \quad (44)$$

$$\phi_n^{\sigma}(x) = x\sigma_{n+1}(x) - (-1)^{\delta_{\sigma,i}} n\sigma_n(x), \quad (45)$$

where δ is the Kronecker delta, $\eta = \sqrt{D_1/D_2}$, $\lambda = s_1 R$, and $\sigma, \upsilon = i, k, j, y$, (i.e., the spherical Bessel functions). We can now start to determine the echo attenuation from Eq. 1. The components of the echo signal are given by

$$\hat{E}_{11}(q, \epsilon) = \frac{1}{a^2 + \lambda^2} - 3 \sum_{n=0}^{\infty} \frac{2n+1}{a^2+\lambda^2} \frac{U_n^i(a, \lambda)W_n^k(a, \eta\lambda)}{\Phi_n(\lambda)}, \quad (46)$$

$$\hat{E}_{12}(q, \epsilon) = 3\eta^2 h_1 \sum_{n=0}^{\infty}(2n+1)\frac{U_n^i(a, \lambda)U_n^k(a, \eta\lambda)}{\Phi_n(\lambda)}, \quad (47)$$

$$\hat{E}_{21}(q, \epsilon) = \frac{\varphi K}{1-\varphi}\hat{E}_{12}(q, \epsilon), \quad (48)$$

and

$$\hat{E}_{22}(q, \epsilon) = \frac{1}{a^2/\eta^2 + \lambda^2} - \frac{3\varphi}{1-\varphi} \sum_{n=0}^{\infty} \frac{2n+1}{a^2/\eta^2+\lambda^2} \frac{U_n^k(a, \eta\lambda)W_n^i(a, \lambda)}{\Phi_n(\lambda)}, \quad (49)$$

where φ is the volume fraction of the spheres in solution,

$$U_n^{\sigma}(a, \lambda) = \frac{\lambda\sigma_{n+1}(\lambda)j_n(a) \pm aj_{n+1}(a)\sigma_n(\lambda)}{(a^2+\lambda^2)\phi_n^{\sigma}(\lambda)}, \quad (50)$$

$$W_n^{\sigma}(a, \lambda) = [1 + \Psi_n^{\sigma}(\lambda)] \times \left\{\left(\mp n + \frac{h_{2,1}}{1+\Psi_n^{\sigma}(\lambda)}\right)j_n(a) \pm aj_{n+1}(a)\right\}, \quad (51)$$

with the upper sign and the first index, i.e., h_2, corresponding to $\sigma = i$ and the lower sign and the second index to $\sigma = k$, respectively, and

$$\Psi_n^{\sigma}(\lambda) = h_{1,2}\sigma_n(\lambda)/\phi_n^{\sigma}(\lambda), \quad (52)$$

$$\Phi_n(\lambda) = 1 + \Psi_n^i(\lambda) + \Psi_n^k(\eta\lambda). \quad (53)$$

Here we have renormalized all parameters to dimensionless form. In particular, time is measured in units of R^2/D_1. All of the echo components are normalized as probabilities in such a way that $E_{11}(0, t) + E_{12}(0, t) = 1$ and $E_{21}(0, t) + E_{22}(0, t) = 1$. NB $E_{ij}(0, t)$ gives the contribution of the spins that have started in phase i and are found in phase j at time t. To calculate the overall echo amplitude, one has to multiply the outer components by a factor of $(1 - \varphi)/\varphi K$ to account for the population difference between the phases. Note that, in the time domain, the first terms in the right-hand side of Eqs. 46 and 49 simply give $\exp(-q^2 Dt)$ for each phase, which is exactly the solution for free diffusion.

Now we have to return to the time domain. Analytical inversion is straightforward but tedious, and eventually reduces to an integration that turns out to be numerically quite intensive. After conducting some comparisons of numerical integration of the inverted solutions to straight numerical inversion of the Laplace transforms of the echo components, we have concluded that numerical inversion is more efficient. Consequently, the results presented below for the two-site microscopic model were obtained by numerical inversion (Stehfest, 1970).

In the case in which one is able to measure the signal from each phase separately, as in the case of hypophosphite

transport in blood cells (Price and Kuchel, 1990b), the following observables are defined:

$$E_1(q, \Delta) = E_{11}(q, \Delta) + \frac{1 - \varphi}{\varphi K} E_{21}(q, \Delta) = E_{11}(q, \Delta) + E_{12}(q, \Delta), \quad (54)$$

$$E_2(q, \Delta) = E_{22}(q, \Delta) + \frac{\varphi K}{1 - \varphi} E_{12}(q, \Delta) = E_{22}(q, \Delta) + E_{21}(q, \Delta), \quad (55)$$

which give the attenuation of the signal due to the spins inside (outside) the cells, respectively.

RESULTS AND DISCUSSION

Macroscopic approach: the Kärger and the modified Kärger models

Some representative curves for the echo attenuation (E) versus q^2 as predicted by the Kärger (i.e., Eqs. 15–18) and the modified Kärger (i.e., Eqs. 15, 21–23) models are presented in Fig. 3. In simulating the plots in Fig. 3, the radius of the spherical interface used was 2.5 μm, and the intracellular diffusion coefficient (D_1) was taken to be 1.5×10^{-10} m^2 s^{-1} (*solid lines* and *filled circles*) or 1.5×10^{-12} m^2 s^{-1} (*dotted line*). These diffusion coefficients correspond to typical values for the real and apparent intracellular diffusion coefficient, respectively, of a small molecule inside a red blood cell (Price and Kuchel, 1990b). When the real intracellular diffusion coefficient is used in the calculations, the Kärger model predicts very fast, almost exponential attenuation, and the agreement with the modified Kärger model is very poor, particularly at larger values of q. When the apparent diffusion coefficient is used in the simulation, the agreement is somewhat better. However, in this case the Kärger model does not accurately predict the diffusion-independent attenuation at large values of q.

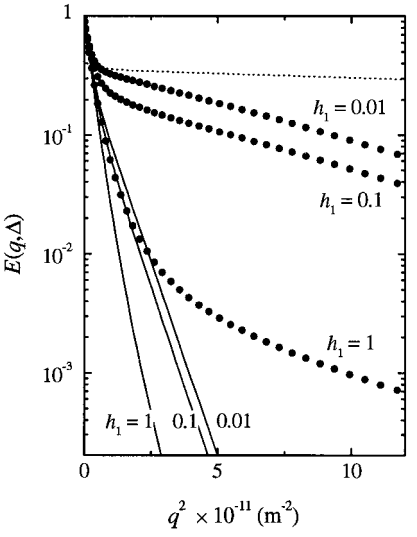

FIGURE 3 Comparison of E versus q^2 for various intracellular lifetimes (τ_1) calculated from the Kärger model (—) and from the modified Kärger model (●●●●). The parameters used in the simulation were consistent with those expected for small metabolite molecules (Price and Kuchel, 1990b). The intracellular and extracellular concentrations were taken to be 41 and 66 mM, respectively, and the volume fractions for the two domains were both taken to be 0.5. Consequently, the internal (P_1) and external (P_2) populations were taken to be 0.38 and 0.62, respectively, and $\Delta = 100$ ms. The extracellular diffusion coefficient (D_2) was taken to be 5.9×10^{-10} m^2 s^{-1}, and the intracellular diffusion coefficient (D_1) was taken to be 1.5×10^{-10} m^2 s^{-1}. When the (unmodified) Kärger model is used to fit the data for such a system, D_1 is generally set to an unphysically small "apparent" value. For comparison one simulation (····) was performed with the Kärger model, in which D_1 was set to 1.5×10^{-12} m^2 s^{-1}. Even though the intracellular lifetime is dependent on D_1, to allow a comparison, the intracellular lifetime was set to the value consistent with $D_1 = 1.5 \times 10^{-10}$ m^2 s^{-1}. The two values for D_1 used correspond to typical values for the real and the (very much smaller) "apparent" diffusion coefficient for a small molecule undergoing restricted diffusion in the intracellular medium. It can be seen that at small q values both the Kärger model and modified Kärger model show good agreement. If the true value for D_1 is used, the Kärger model predicts too rapid decay of the echo signal, whereas if the "apparent" value for D_1 is used, it fails to predict the diffusion-independent signal attenuation.

Microscopic approach: the two-site SGP model

We now turn to a more realistic model that much more closely follows our experimental conditions. Before illustrating the results, we must understand the structure of the expressions for the echo components obtained. Let us consider $E_{11}(q, \Delta)$, for instance. In most cases of practical importance, we can safely assume that $h_1 < 0.1$. Under this condition, the spins that started their motion from inside the sphere are likely to cross the interface only after having diffused for a period sufficient to have thoroughly probed the whole inner space of the spherical interface. It means that the time and q dependence of $E_{11}(q, \Delta)$ can be separated, to a good approximation. The q-behavior of $E_{11}(q, \Delta)$ should be practically the same as that predicted by the one-site model. Basically, the main difference between the one- and two-site models in defining $E_{11}(q, \Delta)$ is that the two-site model takes into account the possibility that a probe leaving a sphere will reenter it after traveling in the external medium. But at low permeability, it is very unlikely that the probe crosses the interface more than once. The dependence on ξ (i.e., on Δ) is governed by $E_{11}(0, \Delta)$, which characterizes the probability that a spin that started its motion from within the sphere will be found in the interior at time Δ. It has been shown (A. V. Barzykin and M. Tachiya, 1998) that at low permeabilities the time behavior of $E_{11}(0, \Delta)$ is well described by a single exponential, i.e., $E_{11}(0, \Delta) \approx \exp(-k_- \Delta)$. The rate constant for exit, k_-, is given by

$$k_- = 3(D_1/R^2)(1/h_1 + \eta^2 K + 1/5)^{-1} \quad (56)$$

or approximately $k_- \approx 3H_1/R$ for low interface permeability. In this sense, our detailed approach provides support for one of the basic assumptions of the Kärger model in the

limit of very low permeability and long Δ. However, the Kärger model also assumes free diffusion in both the internal and external domains that the probes are transported between. As a result, in Eq. 15 Δ appears together with q^2 in the exponent, which is characteristic of free diffusion (see Eq. 5). We will deal with approximate solutions in more detail elsewhere.

A plot of the normalized internal echo amplitude $E_1(q, \Delta)$ as a function of a^2 is shown in Fig. 4 for a few values of the permeability coefficient h_1. The parameters used in the calculations have been chosen to model a typical experiment. We can see how sensitive the model is to permeability changes. This increased sensitivity is due to the contribution from the spins transported through the interface from outside the sphere. At high values of q, when these faster diffusing spins are attenuated, the decay behavior is totally described by $E_{11}(q, \Delta)$, or approximately by the one-site model, which shows only a feeble dependence on the interface permeability. It is the amplitude of the final stage, $E_{11}(0, \Delta)$, that is sensitive to h_1 (see Fig. 5), but this is normalized out in the one-site model.

Correlations and limitations of the macroscopic and microscopic approaches

As mentioned in the Introduction, the application of Kärger's two-site exchange model (Kärger et al., 1988) to systems containing a restricted geometry involves a serious approximation. Because the space coordinate is applied in a macroscopic sense, leaving the space unit much larger than the diameters of the individual domains, this model will fail when Δ is too short to allow for "equilibration" between the different domains. This situation is analogous to the "pore equilibration" assumption (Coy and Callaghan, 1994) in diffusive diffraction experiments. A comparison between the modified Kärger model and the exact model developed in the present work is given in Fig. 6. The discrepancy increases significantly with increasing permeability. However, it must be noted that the modified Kärger model still provides a very good approximation in the long-time limit.

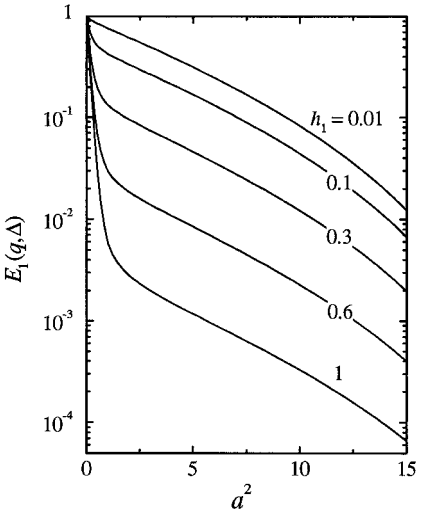

FIGURE 4 Plots of $E_1(q, \Delta)$ versus a^2 for several different values of the (outward) permeability h_1. The calculations were performed using numerical inversion of Eq. 54, with $D_1 = 1.5 \times 10^{-10}$ m^2 s^{-1} and $D_2 = 5.9 \times 10^{-10}$ m^2 s^{-1}. The other parameters are the same as given in the caption to Fig. 3. The behavior of $E_1(q, \Delta)$ is further clarified in Fig. 5.

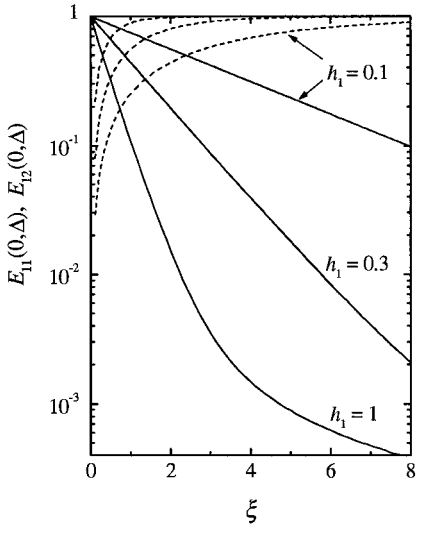

FIGURE 5 Plots of $E_{11}(0, \Delta)$ (—) *and* $E_{12}(0, \Delta)$ (· · · ·) versus ξ for several different values of the (outward) permeability h_1. The lines were calculated using numerical inversion of Eq. 54. The parameters used in the simulations are given in the captions to Figs. 3 and 4. From the plot it can clearly be seen that at low values of h_1 the attenuation appears to be exponential; however, at higher values of h_1 the attenuation is distinctly nonexponential, with an initial rapid decrease followed by a much slower attenuation.

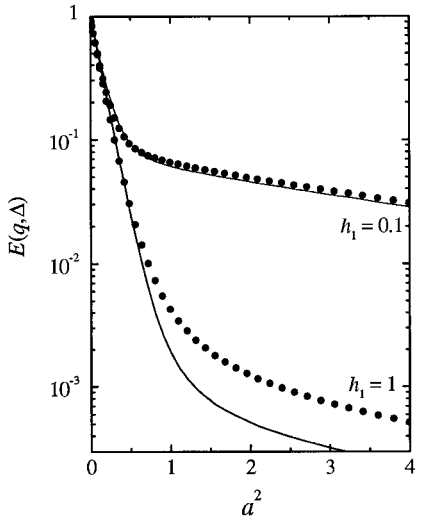

FIGURE 6 Comparison of the total echo attenuation (i.e., $E = E_1 + E_2$; —) calculated from the exact SGP solution with the modified Kärger model (●●●●) versus a^2 for different values of the permeability. The parameters used in the simulations are given in the captions to Figs. 3 and 4. In the calculations φ was set to the relatively low value of 0.2. It is clearly seen that the "exact" solution and the modified Kärger model show some discrepancy at higher permeability values.

A particular advantage of the modified Kärger model is its mathematical simplicity.

Validity of the models to the analysis of experimental PFG transport data

To highlight the strengths, weaknesses, and limitations of the models developed in the present paper, we consider their application to the analysis of a real experimental system in which hypophosphite transport across red blood cell membranes was studied by using PFG NMR measurements (Price and Kuchel, 1990a). Although the experimental parameters used in that study do not sufficiently conform to the SGP limit (operationally $\delta \ll \Delta$) to allow the experimental data to be meaningfully fitted by the theory developed, useful insights can be gained by considering its applicability.

An obvious criticism of applying the above models to real systems is that in real systems, such as blood cells, there is normally a distribution of sizes and the cells are not perfectly spherical. However, it is only in special cases that these nonspherical shapes are aligned (e.g., see Kuchel et al., 1997), and generally their orientation is totally random; thus, especially at low permeabilities and in the (experimentally relevant) long-time limit, the spherical model, where the radius is taken to be that of a sphere of average equivalent volume, is a reasonably good and practical picture of the system.

Because the (NMR) lifetime of the spins in the external domain is not limited, if the restricting geometries have sufficiently high volume fraction, it is possible for a transported species to leave one restricting geometry and then enter another. That is, we cannot consider the effects of each sphere on diffusion completely independently of the other spheres and, thus, in reality we have a many-body problem. Given the true extracellular diffusion coefficient of 1.6×10^{-9} m^2 s^{-1} for a hypophosphite ion, as measured in a cell-free supernatant sample, the mean displacement (i.e., $\sqrt{6D\Delta}$; see Eq. 6) is estimated to be $\sim$30 μm when $\Delta =$ 100 ms. In the present experimental sample, the hematocrit was $\sim$0.7. It follows, then, that a probe can collide with several cells during the time between gradient pulses. It does not necessarily mean, however, that it will be transported across the membrane. When the interface permeability is low, as observed in most cases, it is very unlikely that a probe, once having left one cell, will cross the membrane again and enter another cell on the time scale of a typical experiment. Moreover, because the extracellular diffusion coefficient is much greater than the intracellular diffusion coefficient and the spins in the external medium then rapidly attenuate (see, for example Fig. 4 in (Price and Kuchel, 1990b)), it is likely that only at very high hematocrits will many-body effects make a significant difference. A possible way to include these effects, at least approximately, can be found in the framework of the cell model (Jönsson et al., 1986) or simulations (Jóhannesson and Halle, 1996).

Collisions of the transported species with cells result in an apparent reduction of the free diffusion coefficient in the external medium. This effect is observed in our experiments with cell-free supernatant with a diffusion coefficient (D) of 1.6×10^{-9} m^2 s^{-1}, whereas in the dinitrostilbene-treated cell suspension (i.e., no exchange), the effective extracellular diffusion coefficient, D_{eff}, was 5.9×10^{-10} m^2 s^{-1} (Price and Kuchel, 1990b). Jönsson et al. (1986) have derived an equation to account for obstruction in a system containing monodisperse spherical particles:

$$D_{\text{eff}} = D/(1 + \varphi/2), \tag{57}$$

where D is the true diffusion coefficient, D_{eff} is the effective diffusion coefficient, and φ is the volume fraction (= hematocrit in the case of cells). From Eq. 57 it can be seen that the effective diffusion coefficient decreases sharply as the volume fraction increases, thus causing the apparent external diffusion coefficient to be closer to the internal diffusion coefficient. In the hypophosphite transport experiment, the red cell suspension had a hematocrit of 0.7 (i.e., $\varphi = 0.7$), and the ratio D_{eff}/D was found to be 0.37, whereas Eq. 57 predicts the ratio to be 0.74. The difference is probably due to the poor approximation of an erythrocyte by a sphere, to the intrinsic deficiency of the cell model assuming regular structure of the solution, as well as to the theoretical limitations of Eq. 57 (Jóhannesson and Halle, 1996). In all of our calculations of transport across the spherical interface on the basis of the two-site model, we have used an experimentally determined value of 5.9×10^{-10} m^2 s^{-1} for the extracellular diffusion coefficient.

In reality, differences in magnetic susceptibility between the interior and exterior of the interface can give rise to magnetic field gradients (i.e., in addition to the applied gradient). For a single sphere in a homogeneous magnetic field, these gradients are inversely proportional to the radius (Glasel and Lee, 1974). In biological systems this effect can be amplified by the presence of paramagnetic substances such as deoxyhemoglobin inside the interface (Perng et al., 1993). However, the size of such an in situ gradient is small compared to the applied gradient (Endre et al., 1984; Price et al., 1989a); consequently, these complications were ignored.

CONCLUDING REMARKS

PFG NMR is an important tool for probing transport in biological systems on the basis of differences in the diffusion coefficient and/or the available space for diffusion between the different sites. With the recent advances in NMR hardware, the experiment is relatively easy to perform; however, the analysis required to extract the transport data is not so straightforward. Analytical solutions for the mathematical models required to relate the spin-echo attenuation to the transport parameters rapidly become intractable for all but the simplest systems (geometries). To make the mathematics more tractable, one can attempt to obtain

the "partially absorbing wall" condition, because in most biological and micellar systems it is possible to introduce relaxation agents into the external medium. However, we have shown that this one-site model is relatively insensitive to transport, and in any case it is normally not possible to attain the required boundary conditions (Price and Kuchel, 1990b; Barzykin et al., 1995). In our previous study (Barzykin et al., 1995) we went one step beyond the partially absorbing wall condition to the case in which a species in the external medium is considered to relax very rapidly, compared with the internal spins, but not instantly. This is more consistent with the physical reality when a relaxation agent is added to the external medium. However, the addition of relaxation agents is a high price to pay for mathematical simplicity. In this paper we have treated the general case in which there is no restriction upon the lifetime of a spin in either domain. Ideally, the present model should be extended to consider the case of obstruction in the outer phase and to relax the SGP condition by, for example, applying the Gaussian phase distribution approximation (e.g., Balinov et al., 1993; Kuchel et al., 1996) or other more recent formalisms (Caprihan et al., 1996; Sheltraw and Kenkre, 1996; Callaghan, 1997). Furthermore, in the present paper we have not investigated the well-known "diffraction effects" that normally occur when the echo signal is attenuated to much less than 1%. That these effects will arise in the physical system studied is clear from the form of the E_{11} component and from the form of E_1 in the modified Kärger model. The diffraction effects and extensions beyond the SGP limit will be considered elsewhere.

APPENDIX

Here we present some details of the derivation for the two-site SGP model. Starting from Eqs. 35–37, we derive the Green's function, using the Laplace transform technique (Carslaw and Jaeger, 1959; Barzykin et al., 1995). For the case of $r_0 \le R$, we let

$$G_{11} = G_{1\infty} + w_1 \tag{A1}$$

and

$$G_{12} = w_2, \tag{A2}$$

where $G_{1\infty}$ is the Green's function in an infinite medium satisfying the initial condition of Eq. 3, and w_i ($i = 1, 2$) are the general solutions of Eq. 35 in different domains vanishing at $t = 0$. The Helmholz equation, in spherical coordinates, for $\hat{w}_i$ is given by

$$\frac{\partial^2 \hat{w}_i}{\partial r^2} + \frac{2}{r}\frac{\partial \hat{w}_i}{\partial r} + \frac{1}{r^2}\frac{\partial}{\partial \mu}\left[(1-\mu^2)\frac{\partial \hat{w}_i}{\partial \mu}\right] - s_i^2 \hat{w}_i = 0, \tag{A3}$$

where $s_i = \sqrt{\epsilon/D_i}$. The solution should be finite at the origin and vanish when $r \to \infty$. Therefore,

$$\hat{w}_1 = \sum_{n=0}^{\infty} A_n P_n(\mu) i_n(s_1 r) \tag{A4}$$

and

$$\hat{w}_2 = \sum_{n=0}^{\infty} A_n P_n(\mu) k_n(s_2 r), \tag{A5}$$

where A_n and B_n are constants.

The response to a unit instantaneous point source at $\{r_0, \theta_0, 0\}$ in an infinite medium is

$$\hat{G}_{1\infty} = \frac{1}{4\pi D_1 \tilde{r}} \exp(-s_1 \tilde{r}), \tag{A6}$$

where $\tilde{r}^2 = r_0^2 + r^2 - 2r_0 r \cos(\theta_0 - \theta)$. By using the addition theorems for Bessel functions (Watson, 1966), Eq. A6 can be expressed in a form suitable for use with spherical polar coordinates:

$$\hat{G}_{1\infty} = \frac{s_1}{2\pi^2 D_1} \sum_{n=0}^{\infty} (2n+1) P_n(\mu_0) P_n(\mu) i_n(s_1 r_<) k_n(s_1 r_>), \tag{A7}$$

where $r_< = \min(r, r_0)$ and $r_> = \max(r, r_0)$. The coefficients A_n and B_n in Eqs. A4 and A5, respectively, are determined from the boundary conditions (i.e., Eqs. 36 and 37). Solving the corresponding algebraic equations, we arrive at Eqs. 39 and 40. Equation 41 is obtained in a similar fashion.

Inversion of the Laplace transform involves complex integration. Let us consider G_{11} as an example. By definition, we have

$$G_{11}(r_0, \mu_0 | r, \mu; t) = \frac{1}{2\pi i} \int_{\sigma - i\infty}^{\sigma + i\infty} e^{\epsilon t} \hat{G}_{11}(r_0, \mu_0 | r, \mu; \epsilon) \mathrm{d}\epsilon. \tag{A8}$$

There is a branch point at $\epsilon = 0$, and thus we have to choose a contour with a cut along the negative real axis. Proceeding in a typical way (Carslaw and Jaeger, 1959) with the use of Cauchy's theorem, we find that the line integral (Eq. A8) can be replaced by a real infinite integral, derived from the integrals along $(-\infty - i0, -0 - i0)$ and $(-0 + i0, -\infty + i0)$, which, in our case, happen to be minus complex conjugate. Changing the variable of integration via $\epsilon = D_1 (x/R)^2 e^{i\pi} = -D_1 (x/R)^2$ so that $s_1 = ix/R$ and $s_2 = i\eta x/R$ for $(-0 + i0, -\infty + i0)$ with $\eta = \sqrt{D_1/D_2}$, and using the properties of the Bessel functions with imaginary argument, i.e., $i_n(iz) = i^n j_n(z)$ and $k_n(iz) = \frac{1}{2}\pi i^{-n}[-j_n(z) + i y_n(z)]$, after lengthy but straightforward algebra, we arrive at

$$G_{11}(r_0, \mu_0 | r, \mu; t) = \frac{h_1 h_2}{2\pi\eta R^3} \sum_{n=0}^{\infty} (2n+1) P_n(\mu_0) P_n(\mu) \int_0^{\infty} \mathrm{d}x\, e^{-(D_1 t/R^2)x^2} \times \frac{j_n(x r_0/R) j_n(x r/R)}{[\Lambda_n^{ij}(x)]^2 + [\Lambda_n^{jy}(x)]^2}, \tag{A9}$$

where $\Lambda_n^{\sigma\nu}(x)$ is defined by Eq. 44. Equation A9 is a continuous analog of Eq. 28. In fact, for low permeability values, the integrand in Eq. A9 takes the form of a series of sharp maxima due to the corresponding minima of the denominator. In this case, integration can be effectively represented by summation.

The next step is to calculate the corresponding contribution to the echo signal. Substituting Eq. A9 into Eq. 1, and using the addition theorem for Bessel functions to expand the exponentials and the orthogonality of the Legendre polynomials, we can perform the integration and obtain the attenuation of the signal from spins that started (i.e., before the first

gradient pulse) their motion from within the sphere and are found in the interior at the end of the second gradient pulse,

$$E_{11}(q, \Delta) = \frac{6h_1h_2}{\pi\eta} \sum_{n=0}^{\infty}(2n + 1)\int_0^{\infty} dx\, e^{-\xi x^2} \times \frac{[U_n^{ij}(a, x)]^2}{[\Lambda_n^{ij}(x)]^2 + [\Lambda_n^{jy}(x)]^2}, \quad \text{(A10)}$$

where $\xi = D_1\Delta/R^2$ and

$$U_n^{ij}(a, x) = \frac{xj_{n+1}(x)j_n(a) - aj_n(x)j_{n+1}(a)}{x^2 - a^2}. \quad \text{(A11)}$$

The expression for the other components of the echo signal can be derived in a similar way.

Permeability is typically rather low for biological interfaces. The integrand thus contains rather sharp maxima, which makes numerical integration rather time consuming. We have calculated Laplace transforms of the echo components by substituting Eqs. 39–41 into Eq. 1 and performing integration with the use of the addition theorem. The results are given by Eqs. 46–49. It is possible to proceed in two ways. In the first way the echo attenuation can be computed by numerically inverting Eqs. 46–49. The other alternative is to use Eq. A10 and the like, which, however, also involve numerical integration. With the exception of cross-checking that the two methods give the same result, we have used numerical inversion of Eqs. 46–49, because it is less computationally demanding.

REFERENCES

Abramowitz, M., and I. A. Stegun. 1970. Handbook of Mathematical Functions. Dover, New York.

Andrasko, J. 1976. Water diffusion permeability of human erythrocytes studied by a pulsed field gradient NMR technique. *Biochim. Biophys. Acta.* 428:304–311.

Andreasson, B., L. Nordenskioeld, and J. Schultz. 1996. Interactions of spermidine and methylspermidine with DNA studied by nuclear magnetic resonance self-diffusion measurements. *Biophys. J.* 70:2847–2856.

Balinov, B., B. Jönsson, P. Linse, and O. Söderman. 1993. The NMR self-diffusion method applied to restricted diffusion. Simulation of echo attenuation from molecules in spheres and between planes. *J. Magn. Reson. A.* 104:17–25.

Barzykin, A. V., W. S. Price, K. Hayamizu, and M. Tachiya. 1995. Pulsed field gradient NMR of diffusive transport through a spherical interface into an external medium containing a relaxation agent. *J. Magn. Reson. A.* 114:39–46.

Barzykin, A. V., and M. Tachiya. 1996. Reaction kinetics in microdisperse systems. *Heterogeneous Chem. Rev.* 3:105–167.

Barzykin, A. V., and M. Tachiya. 1998. Diffusive transport across an interface. *J. Phys. Chem.* In press.

Blees, M. H., and J. C. Leyte. 1994. The effective translational self-diffusion coefficient of small molecules in colloidal crystals of spherical particles. *J. Colloid Interface Sci.* 166:118–127.

Callaghan, P. T. 1984. Pulsed field gradient nuclear magnetic resonance as probe of liquid state molecular organization. *Aust. J. Phys.* 37:359–387.

Callaghan, P. T. 1991. Principles of Nuclear Magnetic Resonance Microscopy. Clarendon Press, Oxford.

Callaghan, P. T. 1995. Pulsed gradient spin echo NMR for planar, cylindrical and spherical pores under conditions of wall relaxation. *J. Magn. Reson. A.* 113:53–59.

Callaghan, P. T. 1997. A simple matrix formalism for spin echo analysis of restricted diffusion under generalized gradient waveforms. *J. Magn. Reson.* 129:74–84.

Callaghan, P. T., and A. Coy. 1992. Evidence for reptational motion and the entanglement tube in semidilute polymer solutions. *Phys. Rev. Lett.* 68:3176–3179.

Callaghan, P. T., A. Coy, D. MacGowan, K. J. Packer, and F. O. Zelaya. 1991. Diffraction-like effects in NMR diffusion of fluids in porous solids. *Nature.* 351:467–469.

Caprihan, A., L. Z. Wang, and E. Fukushima. 1996. A multiple-narrow-pulse approximation for restricted diffusion in a time-varying field gradient. *J. Magn. Reson. A.* 118:94–102.

Carslaw, H. S., and J. C. Jaeger. 1959. Conduction of Heat in Solids. Oxford University Press, Oxford.

Chapman, B. E., K. Kirk, and P. W. Kuchel. 1986. Bicarbonate exchange kinetics at equilibrium across the human erythrocyte membrane by ^{13}C NMR. *Biochem. Biophys. Res. Commun.* 136:266–272.

Cory, D. G., and A. N. Garroway. 1990. Measurement of translational displacement probabilities by NMR: an indicator of compartmentation. *Magn. Reson. Med.* 14:435–444.

Coy, A., and P. T. Callaghan. 1994. Pulsed gradient spin echo nuclear magnetic resonance for molecules diffusing between partially reflecting rectangular barriers. *J. Chem. Phys.* 101:4599–4609.

Coy, A., and P. T. Callaghan. 1994. Pulsed gradient spin-echo NMR "diffusive diffraction" experiments on water surrounding close-packed polymer spheres. *J. Colloid Interface Sci.* 168:373–379.

Endre, Z. H., B. E. Chapman, and P. W. Kuchel. 1984. Cell-volume dependence of ^1H spin-echo NMR signals in human erythrocyte suspensions. The influence of in situ field gradients. *Biochim. Biophys. Acta.* 803:137–144.

Fourel, I., J. P. Guillement, and D. Le Botlan. 1994. Determination of water droplet size distributions by low resolution PFG-NMR. *J. Colloid Interface Sci.* 164:48–53.

Frey, S., J. Kärger, H. Pfeifer, and P. Walther. 1988. NMR self-diffusion measurements in regions confined by "absorbing" walls. *J. Magn. Reson.* 79:336–342.

Glasel, J. A., and K. H. Lee. 1974. On the interpretation of water nuclear magnetic resonance relaxation times in heterogeneous systems. *J. Am. Chem. Soc.* 96:970–978.

Jóhannesson, H., and B. Halle. 1996. Solvent diffusion in ordered macrofluids: a stochastic simulation study of the obstruction effect. *J. Chem. Phys.* 104:6807–6817.

Jönsson, B., H. Wennerström, P. G. Nilsson, and P. Linse. 1986. Self-diffusion of small molecules in colloidal systems. *Colloid Polym. Sci.* 264:77–88.

Kärger, J., and W. Heink. 1983. The propagator representation of molecular transport in microporous crystallites. *J. Magn. Reson.* 51:1–7.

Kärger, J., H. Pfeifer, and W. Heink. 1988. Principles and applications of self-diffusion measurements by nuclear magnetic resonance. *Adv. Magn. Reson.* 12:1–89.

Krishnan, V. V. 1997. Determination of oligomeric state of proteins in solution from pulsed-field-gradient self-diffusion coefficient measurements. A comparison of experimental, theoretical, and hard-sphere approximated values. *J. Magn. Reson.* 124:468–473.

Kuchel, P. W. 1990. Spin-exchange NMR spectroscopy in studies of the kinetics of enzymes and membrane transport. *NMR Biomed.* 3:102–119.

Kuchel, P. W., B. T. Bulliman, B. E. Chapman, and K. Kirk. 1987. The use of transmembrane differences in saturation transfer for measuring fast membrane transport: $H^{13}CO_3^-$. *J. Magn. Reson.* 74:1–11.

Kuchel, P. W., A. Coy, and P. Stilbs. 1997. NMR "diffusion-diffraction" of water revealing alignment of erythrocytes in a magnetic field and their dimensions and membrane transport characteristics. *Magn. Reson. Med.* 37:637–643.

Kuchel, P. W., A. J. Lennon, and C. J. Durrant. 1996. Analytical solutions and simulations for spin-echo measurements of diffusion of spins in a sphere with surface and bulk relaxation. *J. Magn. Reson. B.* 112:1–17.

Lennon, A. J., N. R. Scott, B. E. Chapman, and P. W. Kuchel. 1994. Hemoglobin affinity for 2,3-biphosphoglycerate in solutions and intact erythrocytes: studies using pulsed-field gradient nuclear magnetic resonance and Monte Carlo simulations. *Biophys. J.* 67:2096–2109.

Mitra, P. P., and P. N. Sen. 1992. Effects of microgeometry and surface relaxation on NMR pulsed-field-gradient experiments: simple pore geometries. *Phys. Rev. B.* 45:143–156.

New, R. R. C. 1990. Introduction. *In* Liposomes: a practical approach. R. R. C. New, editor. IRL Press, Oxford. 1–32.

Perng, W.-C., W. S. Price, K. Hsu, and L.-P. Hwang. 1993. The effects of hypothermia on the intracellular pH of erythrocytes studied using phosphorus-31 NMR and endogenous compounds. *Eur. J. Clin. Chem. Clin. Biochem.* 31:413–418.

Potter, K., R. L. Kleinberg, F. J. Brockman, and E. W. McFarland. 1996. Assay for bacteria in porous media by diffusion-weighted NMR. *J. Magn. Reson. B.* 113:9–15.

Price, W. S. 1996. Gradient NMR. *In* Annual Reports on NMR Spectroscopy. G. A. Webb, editor. Academic Press, London. 51–142.

Price, W. S. 1997. Pulsed field gradient NMR as a tool for studying translational diffusion. Part 1. Basic theory. *Concepts Magn. Reson.* 9:299–336.

Price, W. S. 1998a. Probing molecular dynamics in biochemical and chemical systems using pulsed field gradient NMR diffusion measurements. *In* Recent Advances in Analytical Techniques. Atta-Ur-Rahman, editor. Gordon and Breach, Amsterdam. In press.

Price, W. S. 1998b. NMR imaging. *In* Annual Reports on NMR Spectroscopy. G. A. Webb, editor. Academic Press, London. In press.

Price, W. S., and Y. Arata. 1996. The manipulation of water relaxation and water suppression in biological systems using the water-PRESS pulse sequence. *J. Magn. Reson. B.* 112:190–192.

Price, W. S., B. E. Chapman, B. A. Cornell, and P. W. Kuchel. 1989a. Translational diffusion of glycine in erythrocytes measured at high resolution with pulsed field gradients. *J. Magn. Reson.* 83:160–166.

Price, W. S., K. Hayamizu, and Y. Arata. 1997a. Optimization of the water-PRESS pulse sequence and its integration into pulse sequences for studying biological molecules. *J. Magn. Reson.* 126:256–265.

Price, W. S., and P. W. Kuchel. 1990a. Hypophosphite transport in human erythrocytes studied by overdetermined one-dimensional NMR exchange analysis. *NMR Biomed.* 3:59–63.

Price, W. S., and P. W. Kuchel. 1990b. Restricted diffusion of bicarbonate and hypophosphite ions modulated by transport in suspensions of red blood cells. *J. Magn. Reson.* 90:100–110.

Price, W. S., P. W. Kuchel, and B. A. Cornell. 1989b. Microviscosity of human erythrocytes studied with hypophosphite and ^{31}P-NMR. *Biophys. Chem.* 33:205–215.

Price, W. S., M. Nara, and Y. Arata. 1997b. A pulsed field gradient NMR study of the aggregation and hydration of parvalbumin. *Biophys. Chem.* 65:179–187.

Price, W. S., B.-C. Perng, C.-L. Tsai, and L.-P. Hwang. 1992. Microviscosity of human erythrocytes studied using hypophosphite two-spin order relaxation. *Biophys. J.* 61:621–630.

Sen, P. N., L. M. Schwartz, P. P. Mitra, and B. I. Halperin. 1994. Surface relaxation and the long-time diffusion coefficient in porous media: periodic geometries. *Phys. Rev. B.* 49:215–225.

Sheltraw, D., and V. M. Kenkre. 1996. The memory-function technique for the calculation of pulsed-gradient NMR signals in confined geometries. *J. Magn. Reson. A.* 122:126–136.

Snaar, J. E. M., and H. Van As. 1993. NMR self-diffusion measurements in a bound system with loss of magnetization at the walls. *J. Magn. Reson. A.* 102:318–326.

Stehfest, H. 1970. Numerical inversion of Laplace transforms. *Commun. ACM.* 13:47–49.

Stejskal, E. O. 1965. Use of spin echoes in a pulsed magnetic-field gradient to study anisotropic restricted diffusion and flow. *J. Chem. Phys.* 43: 3597–3603.

Stejskal, E. O., and J. E. Tanner. 1965. Spin diffusion measurements: spin echoes in the presence of a time-dependent field gradient. *J. Chem. Phys.* 42:288–292.

Stilbs, P. 1987. Fourier transform pulsed-gradient spin-echo studies of molecular diffusion. *Prog. NMR Spectrosc.* 19:1–45.

Torrey, H. C. 1956. Bloch equations with diffusion terms. *Phys. Rev.* 104:563–565.

Van Den Enden, J. C., D. Waddington, H. Van Aalst, C. G. Van Kralingen, and K. J. Packer. 1990. Rapid determination of water droplet size distributions by PFG-NMR. *J. Colloid Interface Sci.* 140:105–113.

Van Zijl, P. C. M., C. T. W. Moonen, P. Faustino, J. Pekar, O. Kaplan, and J. S. Cohen. 1991. Complete separation of intracellular and extracellular information in NMR spectra of perfused cells by diffusion-weighted spectroscopy. *Proc. Natl. Acad. Sci. USA.* 88:3228–3232.

Waldeck, A. R., P. W. Kuchel, A. J. Lennon, and B. E. Chapman. 1997. NMR diffusion measurements to characterise membrane transport and solute binding. *Prog. NMR Spectrosc.* 30:39–68.

Wassall, S. R. 1996. Pulsed field gradient-spin echo NMR studies of water diffusion in a phospholipid model membrane. *Biophys. J.* 71: 2724–2732.

Watson, G. N. 1966. A treatise on the theory of bessel functions. Cambridge University Press, Cambridge.

Zwanzig, R., and A. Szabo. 1991. Time dependent rate of diffusion-influenced ligand binding to receptors on cell surfaces. *Biophys. J.* 60:671–678.